Proc. Natl. Acad. Sci. USA
Vol. 93, pp. 9893–9898, September 1996
Neurobiology

Bcl-2 potentiates the maximal calcium uptake capacity of neural cell mitochondria

(mitochondrial respiration/electron transport chain/ischemia/apoptosis)

ANNE N. MURPHY*†, DALE E. BREDESEN‡, GINO CORTOPASSI§, ENDI WANG§, AND GARY FISKUM*

*Department of Biochemistry and Molecular Biology, The George Washington University Medical Center, Washington, DC 20037; ‡Program on Aging, The Burnham Institute, 10901 North Torrey Pines Road, La Jolla, CA 92037; and §Department of Molecular Biosciences, 1311 Haring Hall, University of California, Davis, CA 95616

Communicated by Louis Sokoloff, National Institutes of Health, Bethesda, MD, June 18, 1996 (received for review January 19, 1996)

ABSTRACT **Expression of the human protooncogene *bcl-2* protects neural cells from death induced by many forms of stress, including conditions that greatly elevate intracellular Ca^{2+}. Considering that Bcl-2 is partially localized to mitochondrial membranes and that excessive mitochondrial Ca^{2+} uptake can impair electron transport and oxidative phosphorylation, the present study tested the hypothesis that mitochondria from Bcl-2-expressing cells have a higher capacity for energy-dependent Ca^{2+} uptake and a greater resistance to Ca^{2+}-induced respiratory injury than mitochondria from cells that do not express this protein. The overexpression of *bcl-2* enhanced the mitochondrial Ca^{2+} uptake capacity using either digitonin-permeabilized GT1-7 neural cells or isolated GT1-7 mitochondria by 1.7 and 3.9 fold, respectively, when glutamate and malate were used as respiratory substrates. This difference was less apparent when respiration was driven by the oxidation of succinate in the presence of the respiratory complex I inhibitor rotenone. Mitochondria from Bcl-2 expressors were also much more resistant to inhibition of NADH-dependent respiration caused by sequestration of large Ca^{2+} loads. The enhanced ability of mitochondria within Bcl-2-expressing cells to sequester large quantities of Ca^{2+} without undergoing profound respiratory impairment provides a plausible mechanism by which Bcl-2 inhibits certain forms of delayed cell death, including neuronal death associated with ischemia and excitotoxicity.**

Expression of the cell death repressor gene *bcl-2* limits the delayed loss of viability initiated by a potentially toxic increase in cytosolic Ca^{2+}, such as that which occurs following ischemia/reperfusion injury (1–4), or treatment of cells with a Ca^{2+} ionophore (5–7). The subcellular mechanism by which Bcl-2 acts is unknown; however, it is has been suggested that Bcl-2 can operate at least indirectly to reduce oxidative processes that may be associated with the death pathway (8–10). Whether this is the sole or direct mechanism of action of Bcl-2 has recently been questioned by data indicating that reactive oxygen species generation is not required for apoptotic death under conditions of very low oxygen tension, and these conditions do not preclude the protective effect of Bcl-2 (11, 12). Other studies directed at identifying a mechanism of action of Bcl-2 have examined the ability of Bcl-2 to affect Ca^{2+} flux within cells. Lam *et al.* (13) have suggested that Bcl-2 inhibits thapsigargin-induced Ca^{2+} efflux from the endoplasmic reticulum. In addition, Baffy *et al.* (14) have reported that following interleukin 3 withdrawal from a cytokine-dependent hematopoietic cell line, Bcl-2 expression inhibited the loss of endoplasmic reticular Ca^{2+} stores and prevented redistribution of Ca^{2+} to the mitochondria.

Protection by Bcl-2 from treatments that result in a substantial rise in cytosolic Ca^{2+} could arise either from effects on the distribution and subcellular levels of intracellular Ca^{2+}, or from effects further downstream through inhibition of Ca^{2+}-mediated events. In general, the ability to withstand a pathological entry of Ca^{2+} into the cell can depend on the activity of several different Ca^{2+} transport processes including that associated with respiration-dependent mitochondrial Ca^{2+} sequestration (15). The mechanisms and potential physiological functions for mitochondrial Ca^{2+} sequestration and efflux have been recently reviewed (15).

The kinetic characteristics of mitochondrial Ca^{2+} uptake and efflux mechanisms dictate that above a threshold concentration of cytosolic Ca^{2+}, mitochondria rapidly accumulate Ca^{2+}, and only slowly release it. As a result, mitochondria have been shown to buffer the increase in cytoplasmic Ca^{2+} concentration in primary cultures of neurons following exposure to the excitatory neurotransmitter glutamate or to depolarization of the plasma membrane (16–19). In response to physiological increases in cytosolic Ca^{2+}, mitochondrial Ca^{2+} uptake may serve as a regulatory mechanism controlling the rate of mitochondrial metabolism and oxidative phosphorylation (15, 20). Under conditions of rapid and prolonged entry of Ca^{2+} into the cytoplasm, which might occur during excitotoxic events or ischemia/reperfusion injury, mitochondria may serve a more significant buffering function and ultimately accumulate large loads of Ca^{2+}. Such net accumulation has been documented during ischemia as well as the early reperfusion phase in models of cerebral, cardiac, and neuronal ischemia (21–24), as well as following excitotoxic challenge to cerebellar granule cells (25). In response to excessive loads, however, mitochondria may incur Ca^{2+}-induced respiratory impairment which compromises the ability of cells to reestablish ionic homeostasis and maintain viable levels of high-energy metabolites such as ATP (23, 26). In fact, prevention of mitochondrial Ca^{2+} sequestration during ischemia using ruthenium red (an inhibitor of the electrophoretic Ca^{2+} uniporter) can be protective to heart tissue (27) and can prevent glutamate-induced excitotoxicity in cerebellar granule cells (25). Ca^{2+}-induced mitochondrial dysfunction may potentiate free radical production (28–30), and exacerbate lactic acidosis, known to play an important role in cell injury following ischemic events. These or potentially other mitochondrial alterations induced by excessive Ca^{2+} sequestration may be critical steps in the apoptotic cell death pathway (31, 32).

The present study has examined the effect of *bcl-2* expression on the ability of mitochondria to sequester high concentrations of extramitochondrial Ca^{2+}. *bcl-2* expression has been found to significantly enhance this uptake capacity, and this

The publication costs of this article were defrayed in part by page charge payment. This article must therefore be hereby marked "*advertisement*" in accordance with 18 U.S.C. §1734 solely to indicate this fact.

†To whom reprint requests should be addressed at: Department of Biochemistry and Molecular Biology, The George Washington University Medical Center, 2300 Eye Street, NW, Washington, DC 20037. e-mail: anmurphy@gwis2.circ.gwu.edu.

potentiation correlates with increased resistance of mitochondria to Ca^{2+}-induced respiratory damage. These data support the hypothesis that the extent of maximal mitochondrial Ca^{2+} sequestration with retention of normal respiratory function can determine the degree of resistance to cell injury related to Ca^{2+} overload.

MATERIALS AND METHODS

Cell Culture. GT1-7 cells, which are immortalized murine hypothalamic neurons (33), were infected with a recombinant retrovirus carrying *bcl-2* and a puromycin resistance gene (pBP-*bcl-2*) or a control retroviral construct as described (8). Positive clones were pooled, and the control (GT1-7*puro*) and *bcl-2* (GT1-7*bcl-2*) transfectants were maintained in poly-L-lysine coated flasks in 5% CO_2/95% air at 37°C in Dulbecco's modified Eagle's medium (DMEM) supplemented with 10% heat inactivated fetal bovine serum (Biofluids, Rockville, MD), 100 units·ml^{-1} penicillin, and 100 $\mu g \cdot ml^{-1}$ streptomycin. PC12 cell transfectants were established and maintained as described (6).

Mitochondrial Isolation. Mitochondria were isolated from cultured cells ($\approx 1 \times 10^9$ cells) essentially by the method of Moreadith and Fiskum (34) with slight modification. Trypsinized cells were centrifuged (85 × *g* for 3 min) in phosphate-buffered saline (137 mM NaCl/2.68 mM KCl/8.1 mM Na_2HPO_4/1.47 mM KH_2PO_4) containing 1 mM EGTA (pH 7.4). The centrifuge tubes were then transferred to ice, and the cells were resuspended and centrifuged again in mitochondrial isolation media (210 mM mannitol/70 mM sucrose/5 mM Hepes/0.5 g of bovine serum albumin per liter/1 mM EGTA, pH 7.2, at 4°C). All subsequent steps of the preparation, including selective permeabilization of the plasma membranes, were performed on ice with media maintained at 4°C as described (34). Measured by atomic absorption (35), the total calcium content of mitochondria isolated from GT1-7*puro* cells was 8.1 nmol/mg protein, and from GT1-7*bcl-2* cells was 6.8 nmol/mg protein. Protein determination was performed with a modified biuret assay (36).

Measurement of Mitochondrial Ca^{2+} Uptake Capacity of Digitonin-Permeabilized Cells or Isolated Mitochondria. Extramitochondrial free Ca^{2+} was monitored in the presence of isolated mitochondria or digitonin-permeabilized cells (see Fig. 1) using the hexapotassium salt of Calcium green-5N (Molecular Probes). This Ca^{2+}-sensitive fluorescent indicator exhibits a K_D for Ca^{2+} of ≈ 4 μM (37), which makes it more suitable for measurement of micromolar concentrations of Ca^{2+} than higher affinity dyes such as fura-2. Isolated mitochondria (0.25 mg·ml^{-1}) were suspended in potassium chloride (KCl) media (125 mM KCl/2 mM K_2HPO_4/1 mM $MgCl_2$/20 mM Hepes, pH 7.0) containing 0.1 μM Calcium green-5N and either 5 mM glutamate and 5 mM malate or 5 mM succinate and 4 μM rotenone. Fluorescence was continuously monitored at 37°C using a Perkin–Elmer LS-3 fluorescence spectrometer equipped with a stirring device with the excitation at 506 nm and emission at 531 nm. Measurement of mitochondrial Ca^{2+} uptake in digitonin-permeabilized cells was performed by first harvesting cells in growth media by trypsinization, followed by centrifugation in growth medium (85 × *g* for 3 min) and resuspension of the cells (2.17×10^7 cells/ml) in KCl medium containing the indicated oxidizable substrate(s) and 0.1 μM Calcium green-5N. The plasma membranes were then selectively permeabilized with a titrated concentration of digitonin [final digitonin, 0.01% (wt/vol)]. The fluorescence values were calibrated by successive addition of known amounts of $CaCl_2$ to medium containing mitochondria or permeabilized cells in which Ca^{2+} uptake was prevented by the addition of 4 μM rotenone or rotenone plus 2.5 $\mu g \cdot ml^{-1}$ oligomycin, respectively. Quantitation of partial uptake of a pulse of Ca^{2+} was done by using the calibration curve to determine the quantity of each pulse that the mitochondria were unable to sequester. This curve is not intended to reflect the medium free Ca^{2+} ion concentrations because a small portion of the added Ca^{2+} may be bound by phosphate in the experimental media or EGTA carried into the assay with the isolated mitochondria. Because of this buffering and the inability of Calcium green-5N to accurately quantitate Ca^{2+} at very low levels (37), the calibration curve is labeled "added Ca^{2+}," indicative of the fluorescence level associated with a known quantity of $CaCl_2$ added to the medium.

Measurement of Respiration by Isolated Mitochondria and Digitonin-Permeabilized Cells. Respiration of isolated mitochondria (0.50 mg/ml; 0.6 ml vol) and digitonin-permeabilized cells (2.17×10^7 cells/ml; 0.6 ml vol) was measured polarographically in KCl media containing 5 mM glutamate and 5 mM malate in a thermostatically controlled (37°C) oxygen electrode chamber (Diamond General, Ann Arbor, MI). For measurement of mitochondrial respiration, the mitochondria were added to the chamber and after 2 min, either 333 nmol $CaCl_2$ mg·protein^{-1} (167 μM) was added to the chamber, or no addition of $CaCl_2$ was made. After another 2 min to allow for Ca^{2+} sequestration, state 3 (phosphorylating) respiration was initiated with the addition of 0.66 mM ADP. State 4 (resting) respiration was then induced by addition of 1.25 $\mu g \cdot ml^{-1}$ oligomycin (Calbiochem). Maximal rates of electron flow through the electron transport chain (state 3_u) were subsequently measured by titration with the uncoupler FCCP (carbonyl cyanide *p*-trifluoromethoxyphenylhydrazone; 80 nM; Calbiochem). For measurement of permeabilized cell respiration, 1.2×10^7 cells were centrifuged, resuspended to 0.6 ml in KCl medium, transferred to the oxygen electrode chamber, and then permeabilized in the presence of glutamate and malate as oxidizable substrates. The indicated amount of Ca^{2+} was then added. After a 5-min incubation to allow the mitochondria to sequester the majority of the added Ca^{2+}, the maximal rates of uncoupler-stimulated respiration were measured by titration with FCCP. Stock solutions of $CaCl_2$ were quantified using atomic absorption spectroscopy (35). The solubility of oxygen in the air saturated medium at 37°C was assumed at 390 ng-atoms O·ml^{-1}.

Measurement of Cytochrome Oxidase Activity and Mitochondrial DNA Content of GT1-7 Cells. Cytochrome *c* oxidase (complex IV) activity was measured spectrophotometrically essentially as described by Smith (38), except that the initial cytochrome *c*(II) concentration was 36 μM. The solution of cytochrome *c* was initially reduced to ferrocytochrome with dithionite. Activity of the enzyme is expressed as nmol cytochrome *c* oxidized·min^{-1}·5×10^5 $cells^{-1}$.

For measurement of mtDNA, GT1-7 transfectants were trypsinized and DNA was extracted by proteinase K digestion in SDS, followed by phenol/chloroform extraction (39); relative quantity and purity of total DNA was determined spectrophotometrically by absorption at 260 and 280 nm. Relative quantities of mtDNA were measured by serial dilution of the DNA pools from *puro* and *bcl-2* cells, followed by PCR using conditions previously described (40), and the following primers: Pf, caagtccatgaccattaactgg; Pr, gggatgtttttaggcttagg. Cycling conditions included an initial 4-min denaturation at 94°C, followed by 30 cycles of denaturation, annealing and extension at 94°C for 20 s, 55°C for 20 s, and 72°C for 20 s, and a final extension at 72°C for 4 min. PCR products were electrophoresed through 1.5% agarose gels stained with ethidium bromide. Band intensities were quantified using the BIOIMAGE program of the MilliGen/Biosearch imaging system. A linear relationship between band intensities and quantity of DNA in the PCR existed when 1.6–12.5 ng DNA was included in the reactions.

RESULTS

Mitochondrial Ca^{2+} Uptake Capacity. Respiration-dependent electrophoretic transport of Ca^{2+} results in rapid net accumulation of ambient Ca^{2+} into mitochondria (15). The

maximal quantity of Ca^{2+} that can be sequestered by mitochondria can be measured by monitoring the disappearance of extramitochondrial free Ca^{2+} from media following the addition of quantified pulses of $CaCl_2$. A typical Calcium green-5N fluorescence tracing measuring the Ca^{2+} uptake capacity of mitochondria isolated from GT1-7*bcl-2* and GT1-7*puro* cells respiring in the presence of 5 mM glutamate and 5 mM malate is shown in Fig. 1 *A* and *B*, respectively. The addition of mitochondria to the medium resulted in a rapid decrease in the free [Ca^{2+}] due to respiration-dependent uptake of contaminating Ca^{2+} ($\approx$6 μM by atomic absorption), as well as due to Ca^{2+} chelation by the contaminating EGTA contained in the aliquot of added mitochondria ($\approx$20 μM). After equilibrium was reached, a pulse of $CaCl_2$ (59 μM = 236 nmol/mg protein) was added as indicated by a rapid rise in dye fluorescence, followed by mitochondrial sequestration of Ca^{2+} from the medium. As seen in Fig. 1*A*, after sequestration of this added Ca^{2+}, the steady-state level of medium Ca^{2+} was slightly higher than the initial steady state due to Ca^{2+} saturation of the contaminating EGTA in the medium. An equivalent amount of $CaCl_2$ was repeatedly added every 2 min until there was no further evidence of Ca^{2+} uptake. Addition of Ca^{2+} after this point was associated with a further increase in fluorescence, indicating that the levels of added Ca^{2+} are subsaturating to the dye under these conditions. As is evident in Fig. 1*A*, mitochondria isolated from GT1-7*bcl-2* cells could sequester a greater number of pulses of Ca^{2+} than those from GT1-7*puro* cells under these conditions. Similar experiments with *bcl-2* and *puro* mitochondria were performed in the presence of the FAD-linked substrate succinate along with the complex I inhibitor rotenone to block utilization of NADH by the electron transport chain. Although the general patterns of Ca^{2+} sequestration were similar to those in the presence of glutamate and malate, the total amount accumulated by *bcl-2* mitochondria was lower and was similar to the amount accumulated by the control (*puro*) mitochondria. The average maximal capacity for Ca^{2+} accumulation of GT1-7*puro* and *bcl-2* mitochondria respiring on either glutamate and malate or succinate in the presence of rotenone is shown in Table 1. When oxidizing glutamate and malate, thereby providing reducing equivalents to the electron transport chain in the form of NADH, GT1-7*bcl-2* mitochondria accumulated almost 4-fold the amount sequestered by GT1-7*puro* mitochondria ($P < 0.001$). However, in the presence of succinate (plus rotenone), the uptake capacity of *bcl-2* was only slightly greater and not statistically different from the amount sequestered by *puro* mitochondria. These results imply a difference in the ability of Bcl-2 to potentiate Ca^{2+} uptake capacity dependent upon the source of reducing equivalents being donated to the electron transport chain.

The Ca^{2+} Uptake Capacity of Digitonin-Permeabilized Cells. In an effort to provide evidence that the enhanced ability of mitochondria isolated from *bcl-2*-expressing cells to accumulate Ca^{2+} in the presence of glutamate and malate was not due to an artifact of the mitochondrial isolation procedure, Ca^{2+} accumulation was also measured using digitonin-permeabilized cells. The plasma membranes of cells can be selectively permeabilized using a titrated amount of digitonin, due to the ability of this steroid glycoside to specifically extract cholesterol and cholesterol esters from membranes with relatively high cholesterol levels (34). As a result, Ca^{2+} transport and respiratory functions of cellular organelles can essentially be measured *in situ* (34, 41) with minimal disruption of the cytoarchitecture (42). Fig. 1 shows a typical fluorescence tracing of Ca^{2+} uptake using digitonin-permeabilized GT1-7*bcl-2* or *puro* cells oxidizing glutamate and malate (Fig. 1 *C* and *D*, respectively). The contribution of endoplasmic reticular Ca^{2+} sequestration to total Ca^{2+} uptake was negligible, as evidenced by the lack of accumulation of added Ca^{2+} in the presence of the mitochondrial respiratory inhibitor, antimycin A (data not shown). Similar to the results using isolated mitochondria in the presence of NAD^+-linked substrates, the average uptake capacity of digitonin-permeabilized GT1-7*bcl-2* cells was significantly greater than that of GT1-7*puro*

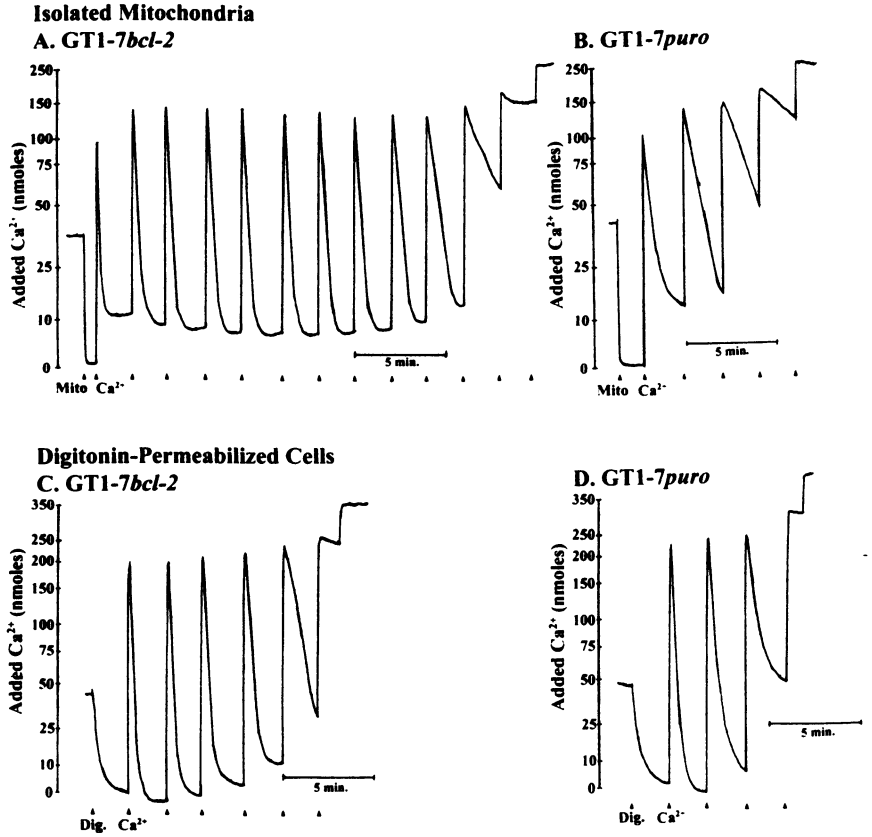

FIG. 1. Fluorescent measurement of Ca^{2+} uptake using isolated mitochondria or digitonin-permeabilized cells. Maximal mitochondrial Ca^{2+} uptake by mitochondria (0.25 mg·ml^{-1} in 2 ml) isolated from GT1-7 *bcl-2* (*A*) and *puro* (*B*) cells in the presence of 5 mM glutamate and 5 mM malate was measured as described using Calcium green-5N as an indicator of the free Ca^{2+} concentration in the medium (506 nm excitation, 531 nm emission). Equivalent pulses of $CaCl_2$ (118 nmol/2 ml = 59 μM) were added to isolated mitochondria every 2 min until there was no longer evidence of uptake of the added Ca^{2+}. The maximal Ca^{2+} uptake during this experiment for *bcl-2* mitochondria (*A*) was 2736 nmol/mg protein and for *puro* mitochondria (*B*) was 756 nmol/mg protein, respectively. For measurement of maximal Ca^{2+} uptake using digitonin-permeabilized cells, intact GT1-7*bcl-2* (*C*) or GT1-7*puro* (*D*) cells (2.17×10^7 cells·ml^{-1} in 2 ml) were added to the KCl media containing glutamate and malate and then digitonin-permeabilized. Pulses of 200 nmol $CaCl_2$ (100 μM) were added every 2 min. Maximal Ca^{2+} uptake for GT1-7*bcl-2* cells was 1110 nmol/5 $\times$ 10^7 cells (*C*) and for GT1-7*puro* was 640 nmol/5 $\times$ 10^7 cells (*D*).

Table 1. Effect of Bcl-2 on the Ca^{2+} uptake capacity of isolated GT1-7 mitochondria and digitonin-permeabilized cells

	Maximal Ca^{2+} uptake			
	Isolated mitochondria, nmol Ca^{2+}·mg·protein^{-1}		Permeabilized cells, nmol Ca^{2+}·5 × 10^7 cells^{-1}	
Oxidizable substrate	GT1-7*puro*	GT1-7*bcl-2*	GT1-7*puro*	GT1-7*bcl-2*
Glutamate + malate	586 ± 118	2287 ± 168*	860 ± 124	1426 ± 126†
Succinate (+ Rot)	587 ± 58	745 ± 78	675 ± 54	1007 ± 59‡

Maximal Ca^{2+} sequestration (± SEM) by isolated mitochondria or digitonin-permeabilized GT1-7*puro* or *bcl-2* cells was measured as shown in Fig. 1 and described in *Materials and Methods* in the presence of glutamate/malate or succinate (+ rotenone) (n = 5–9).
*Significantly different from GT1-7*puro* Ca^{2+} accumulation by isolated mitochondria in the presence of glutamate and malate by Student's t test ($P < 0.001$).
†Significantly different from GT1-7*puro* cells oxidizing glutamate and malate ($P = 0.007$).
‡Significantly different from GT1-7*puro* cells oxidizing succinate ($P = 0.002$).

cells; however, this difference was not as great as with isolated mitochondria (Table 1). Maximal Ca^{2+} sequestration by permeabilized *bcl-2* cells was also slightly greater in the presence of succinate plus rotenone (Table 1). In contrast to the data with isolated mitochondria, this difference was statistically significant with permeabilized cells ($P = 0.002$).

The results indicating Bcl-2 enhancement of the Ca^{2+} uptake capacity of digitonin-permeabilized cells could arise simply from an elevated number of mitochondria in GT1-7*bcl-2* cells. Therefore, indirect measures of mitochondrial quantity in GT1-7*puro* and *bcl-2* cells were made by assessing the level of cytochrome oxidase activity (complex IV of the electron transport chain) in extracts of GT1-7 transfectants, as well as by measuring mtDNA content. Cytochrome oxidase activity was statistically similar in extracts of the two cell types: 7.25 ± 0.65 (SEM) and 8.67 ± 0.83 nmol·min^{-1}·5 × 10^5 cells^{-1} for GT1-7*puro* and *bcl-2* cells, respectively (n = 5). Also, the amount of mtDNA per microgram of total DNA was similar as evidenced by the density of ethidium bromide-stained bands normalized to 12.5 ng DNA in the PCR [9.47 ± 0.54 units (SEM) for *puro* versus 10.18 ± 0.45 units for *bcl-2* (n = 4)]. Combined, these results indicate that the enhanced Ca^{2+} uptake capacity of digitonin-permeabilized GT1-7*bcl-2* cells was not the result of an increased mitochondrial copy number compared with *puro* controls. In further support, experiments with digitonin-permeabilized cells like those of Fig. 1 *C* and *D* using similarly transfected PC12 cells have indicated that the maximal Ca^{2+} uptake capacity of *bcl-2* overexpressors (439 ± 72 nmol/5 × 10^7 cells SEM) is significantly greater than that of control transfectants (202 ± 61; n = 4; $P < 0.05$). These results suggest that the effect of *bcl-2* expression on mitochondrial Ca^{2+} sequestration is not unique to GT1-7 cells.

The Ca^{2+}Sensitivity of Mitochondrial Respiration. If an increased capacity to accumulate Ca^{2+} is to serve a protective function to the cell, it should coincide with an enhanced ability to withstand Ca^{2+}-induced damage to mitochondrial respiratory function (43). Therefore, the sensitivity of respiratory rates of isolated mitochondria to high concentrations of Ca^{2+} added to media containing glutamate and malate was measured (Table 2). Oxygen consumption during state 3 (ADP phosphorylating) respiration is indicative of the concurrent functions of substrate oxidation, electron transport, the ATP synthetase, the adenine nucleotide translocase, and the phosphate transporter. The rate of uncoupler stimulated respiration (state 3_u) is a clearer indicator of the maximal rate of electron transport due to the removal of potential rate restrictions imposed by the ATP synthetase and transporters. The extent of mitochondrial respiratory inhibition of both state 3 and state 3_u rates in response to incubation in the presence of 333 nmol Ca^{2+}/mg protein was significantly greater for GT1-7*puro* mitochondria than *bcl-2* mitochondria ($P = 0.015$). Although mitochondrial Ca^{2+} overload can result in an uncoupling effect that would be expected to elevate the resting level of respiration (43), the rates of resting (state 4) respiration remained relatively unchanged in response to this concentration of added Ca^{2+} (Table 2).

Similar to the approach for measurement of Ca^{2+} uptake capacities, the susceptibility of GT1-7*puro* and *bcl-2* respiration to Ca^{2+}-induced inhibition was also assessed using digitonin-permeabilized cells. As shown in Fig. 2, the rates of glutamate/malate-dependent uncoupler-stimulated respiration were measured at three levels of added Ca^{2+}. With the lowest amount of added Ca^{2+} (385 nmol/5 × 10^7 permeabilized cells), which was a level below the maximal Ca^{2+} uptake capacity of either cell type (see Table 1), the uncoupler-stimulated rates of GT1-7*puro* and *bcl-2* cells were similar to one another and similar to controls for which no Ca^{2+} was added. In response to an intermediate Ca^{2+} load (960 nmol/5 × 10^7 cells) which was slightly above the maximal capacity of the control cells (Table 1), Bcl-2 expression provided significant protection from Ca^{2+}-induced inhibition evident in permeabilized GT1-7*puro* cells ($P < 0.05$). The respiration of both

Table 2. Bcl-2 provides protection from Ca^{2+}-induced respiratory inhibition to isolated mitochondria

		Mitochondrial respiratory rate, ng atoms O·min^{-1}·mg protein^{-1}		
Cell type	Added Ca^{2+}	State 3	State 4	State 3_u
GT1-7*puro*	−	55.0 ± 6.6	16.1 ± 1.0	85.2 ± 12.7
	+	17.8 ± 1.4 (67±2%)*	14.3 ± 0.4	29.7 ± 2.1 (63±7%)
GT1-7*bcl-2*	−	103.0 ± 6.7	26.2 ± 3.6	186.0 ± 28.5
	+	53.8 ± 5.0 (47±6%)	29.7 ± 1.0	117.2 ± 4.6 (32±11%)

Mitochondrial respiratory rates (±SEM) in the presence of glutamate and malate was measured as described in *Materials and Methods*. Added Ca^{2+} refers to either the omission (−) or addition (+) of 333 nmols $CaCl_2$·mg^{-1} protein (167 μM). State 3_u refers to the maximal uncoupler-stimulated respiration. The percent inhibition of the state 3 and state 3_u rates with respect to the rates in the absence of added Ca^{2+} is indicated parenthetically (n = 4).
*Student's t test indicated that the percent inhibition of GT1-7*puro* state 3 was significantly greater than that for GT1-7*bcl-2* ($P = 0.015$).

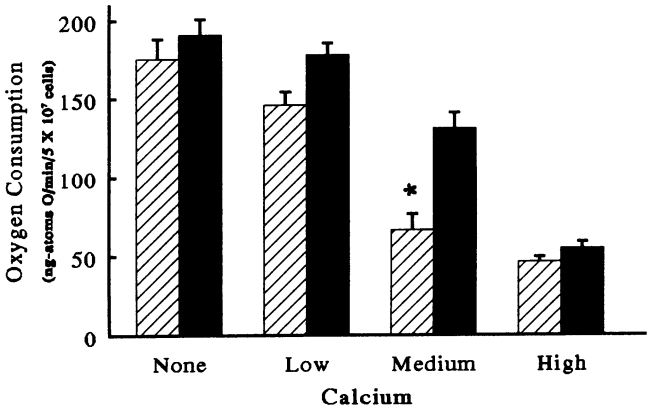

FIG. 2. Rates of uncoupler-stimulated respiration of digitonin-permeabilized GT1-7*puro* (hatched bars, ±SEM) or GT1-7*bcl-2* cells (solid bars) incubated in the presence of 5 mM glutamate and 5 mM malate were measured following no addition of Ca^{2+} (none), or the addition of low (167 μM, equivalent to 385 nmol $CaCl_2/5 \times 10^7$ cells), medium (417 μM, equivalent to 960 nmol $CaCl_2/5 \times 10^7$ cells), or high levels of $CaCl_2$ (833 μM, equivalent to 1925 nmol $CaCl_2/5 \times 10^7$ cells) as described in *Materials and Methods*. *, Two-way analysis of variance detected an interaction of cell type and Ca^{2+} level. The rate of GT1-7*bcl-2* respiration in response to 960 nmol $CaCl_2/5 \times 10^7$ cells was significantly greater than that of GT1-7*puro* at the same Ca^{2+} load ($P = 0.04$) by post hoc F-test ($n = 6$–7).

cell types was severely inhibited at the highest Ca^{2+} concentration tested (1925 nmol/5×10^7 cells), which was beyond the maximal capacity of both cells types (Table 1), demonstrating that the protection of respiratory function by Bcl-2 can be overcome by excessive Ca^{2+} sequestration.

DISCUSSION

Providing a potential mechanism of action of *bcl-2* protection in response to cellular Ca^{2+} overload, these data indicate that Bcl-2 potentiates maximal Ca^{2+} sequestration by mitochondria and can inhibit Ca^{2+}-induced respiratory damage that can be associated with accumulation of high levels of Ca^{2+}. Thus, the ability of mitochondria within *bcl-2* expressing cells to maintain normal functional integrity in response to potentially toxic levels of extramitochondrial Ca^{2+} may contribute to the mechanism(s) by which Bcl-2 provides resistance to delayed cell death such as that which follows cerebral ischemia. Mitochondria can buffer the peak Ca^{2+} values in response to elevations induced by NMDA receptor activation or cell depolarization (16–19). Hartley *et al.* (44) have suggested that the total entry of Ca^{2+} correlates better with viability than measured free Ca^{2+} values, suggesting that the noncytosolic Ca^{2+} loads are important to the regulation of the cell death pathway. Maintenance of normal respiratory electron flow following periods of high cytosolic Ca^{2+} concentrations is critical not only to continued ATP production, but also to avoid Ca^{2+}-potentiation of mitochondrial superoxide generation (28, 45, 46). This Ca^{2+}-induced event may have particular relevance in neuronal cells, in which NMDA receptor activation has been shown to result in reactive oxygen species generation (29, 30, 47) consistent with a mitochondrial source (29, 30). Studies of mitochondrial free radical generation have indicated that ischemia- or chemical-induced inhibition of electron transport can potentiate reactive oxygen species production (28, 46, 48–50). Therefore, resistance to Ca^{2+}-induced inhibition may prevent an increase in mitochondrial free-radical production, which can, in turn, be exacerbated by feed-forward mechanisms (28). It is also possible that Bcl-2 confers mitochondria with resistance to forms of stress other than elevated Ca^{2+}, including direct oxidative stress.

Baffy *et al.* (14) have reported that an elevated mitochondrial pool of Ca^{2+} is associated with control but not *bcl-2* overexpressing hematopoietic cells challenged with cytokine withdrawal. Elevations in cytosolic Ca^{2+} were not evident under these conditions, suggesting that cytokine withdrawal is associated with an enhanced affinity for Ca^{2+} (a lower buffer point) of the mitochondria in the control but not the *bcl-2*-expressing cells. The current data address the maximal Ca^{2+} uptake capacity, which is distinct from the mitochondrial Ca^{2+} buffer point. Together these data predict that at lower cytosolic Ca^{2+} levels, Bcl-2 maintains the buffer point at a level that avoids Ca^{2+} sequestration, and at high cytosolic Ca^{2+} levels Bcl-2 will allow greater sequestration with avoidance of respiratory damage.

Beyond the primary observations of increased Ca^{2+} uptake capacities and resistance to Ca^{2+}-induced respiratory inhibition conferred by Bcl-2, these data provide the intriguing finding that Bcl-2 potentiates Ca^{2+} uptake capacity when isolated mitochondria are oxidizing the NAD^+-linked substrates, glutamate and malate, yet Bcl-2 has no significant effect on maximal Ca^{2+} uptake when the FAD-linked substrate succinate is provided. Although Bcl-2 did enhance succinate-dependent maximal Ca^{2+} sequestration by digitonin-permeabilized cells (Table 1) and had a slight (although not statistically significant) enhancing effect on isolated mitochondria oxidizing succinate, it is clear that the enhancement by Bcl-2 of the maximal uptake capacity is greater when the mitochondria are oxidizing glutamate and malate versus succinate. One interpretation of these data is that NAD^+-linked substrates are necessary for potentiation by Bcl-2 of maximal Ca^{2+} sequestration. If this is true, then Bcl-2 activity may require either generation (or preservation) of mitochondrial NAD(P)H, or activity of complex I of the electron transport chain. If preservation of NAD(P)H is the critical activity, then residual endogenous substrates may account for the lack of a difference in succinate-dependent uptake when using digitonin-permeabilized cells. Another related interpretation is that in the presence of succinate (plus rotenone), degradative mechanisms stimulated by Ca^{2+} sequestration overwhelm the protective action of Bcl-2. These assays provide a subcellular system in which to further investigate the mechanism of Bcl-2 action.

A number of studies have documented mitochondrial alterations in the pathway of delayed death (10, 51–56, 63). Whether these alterations are causative or a consequence of activation of the death pathway is unclear (see ref. 32 for a review). However, using reconstitution assays for apoptosis, several studies have implicated the mitochondrial fraction, or a component thereof, as responsible for induction of nuclear disintegration (31, 64), and activation of the interleukin 1β-converting enzyme (ICE) family protease member CPP32 (65), providing compelling evidence that an alteration in mitochondrial function is critical in triggering apoptosis. The nature of such an alteration involved in the induction of the death pathway is unknown, but may arise from severe respiratory inhibition, loss in the membrane potential, the opening of the mitochondrial membrane permeability transition pore (15, 57–59, 64) or the loss of cytochrome *c* from the intermembrane space (65). Pore opening may be associated the with oxidation and subsequent degradation or loss of pyridine nucleotides (60, 66), which may relate to the current results of substrate-dependent potentiation of Ca^{2+} uptake capacity. Mitochondrial swelling and release of cytochrome *c* have long been known to accompany respiratory alterations induced by extensive Ca^{2+} sequestration (67). Preliminary results indicate that 20 μM cyclosporin A (Sandoz Pharmaceuticals), an inhibitor of the permeability transition, increases the maximal Ca^{2+} uptake capacity of both GT1-7*puro* and *bcl-2* permeabilized cells; however, the uptake capacity of GT1-7*bcl-2* cells was still 1.3- to 1.8-fold greater than control cells. Bcl-2 expression has been reported to elevate the mitochondrial membrane potential (62) and shift the cellular redox state of pyridine nucleotides, protein sulhydryls, and glutathione to a

more reduced level (63), but how these observations relate to resistance to either the probability of mitochondrial pore opening or to the current data will require further investigation.

We are indebted to Stephen J. Russell and Mary Lee for their expert technical assistance, and to Ian J. Reynolds, Ph.D. for his critical reading of this manuscript. This work was supported by National Institutes of Health Grants NS 34152 to GF and AG12282 to D.E.B., and by the Souer's Stroke Fund at George Washington University Medical Center.

1. Martinou, J.-C., Dubois-Dauphin, M., Staple, J. K., Rodriguez, I., Frankowski, H., Missotten, M., Albertini, P., Talabot, D., Catsicas, S., Pietra, C. & Huarte, J. (1994) *Neuron* **13,** 1017–1030.
2. Linnik, M. D., Zahos, P., Geschwind, M. D. & Federoff, H. J. (1995) *Stroke* **26,** 1670–1675.
3. Shimazaki, K., Ishida, A. & Kawai, N. (1994) *Neurosci. Res.* **20,** 95–99.
4. Chen, J., Graham, S. H., Chan, P. H., Lan, J. & Simon, R. P. (1995) *NeuroReport* **6,** 394–398.
5. Zhong, L.-T., Sarafian, T., Kane, D. J., Charles, A. C., Mah, S. P., Edwards, R. H. & Bredesen, D. E. (1993) *Proc. Natl. Acad. Sci. USA* **90,** 4533–4537.
6. Mah, S. P., Zhong, L. T., Liu, Y., Roghani, A., Edwards, R. H. & Bredesen, D. E. (1993) *J. Neurochem.* **60,** 1183–1186.
7. Caron-Leslie, L.-U. M., Evans, R. B. & Cidlowski, J. A. (1994) *FASEB J.* **8,** 639–645.
8. Kane, D. J., Sarafian, T. A., Anton, R., Hahn, H., Gralla, E. B., Valentine, J. S., Örd, T. & Bredesen, D. E. (1993) *Science* **262,** 1274–1277.
9. Hockenbery, D. M., Oltvai, Z. N., Yin, X.-M., Milliman, C. L. & Korsmeyer, S. J. (1993) *Cell* **75,** 241–251.
10. Myers, K. M., Fiskum, G., Liu, Y., Simmens, S. J., Bredesen, D. E. & Murphy, A. N. (1995) *J. Neurochem.* **65,** 2432–2440.
11. Jacobson, M. D. & Raff, M. C. (1995) *Nature (London)* **374,** 814–816.
12. Shimizu, S., Eguchi, Y., Kosaka, H., Kamiike, W., Matsuda, H. & Tsujimoto, Y. (1995) *Nature (London)* **374,** 811–813.
13. Lam, M., Dubyak, G., Chen, L., Nunez, G., Miesfeld, R. L. & Distelhorst, C. W. (1994) *Proc. Natl. Acad. Sci. USA* **91,** 6569–6573.
14. Baffy, G., Miyashita, T., Williamson, J. R. & Reed, J. C. (1993) *J. Biol. Chem.* **268,** 6511–6519.
15. Gunter, T. E., Gunter, K. K., Sheu, S.-S. & Gavin, C. E. (1994) *Am. J. Physiol.* **267,** C313–C339.
16. Tatsumi, H. & Katayama, Y. (1993) *J. Physiol. (London)* **464,** 165–181.
17. Werth, J. L. & Thayer, S. A. (1994) *J. Neurosci.* **14,** 348–356.
18. White, R. J. & Reynolds, I. J. (1995) *J. Neurosci.* **15,** 1318–1328.
19. Budd, S. L. & Nicholls, D. G. (1996) *J. Neurochem.* **66,** 403–411.
20. Murphy, A. N., Kelleher, J. K. & Fiskum, G. (1990) *J. Biol. Chem.* **265,** 10527–10534.
21. Allen, S. P., Darley-Usmar, V. M., McCormack, J. G. & Stone, D. (1993) *J. Mol. Cell. Cardiol.* **25,** 949–958.
22. Zaidan, E. & Sims, N. R. (1994) *J. Neurochem.* **63,** 1812–1819.
23. Sun, D. & Gilboe, D. D. (1994) *J. Neurochem.* **62,** 1921–1928.
24. LoPachin, R. M., Jr., & Stys, P. K. (1995) *J. Neurosci.* **15,** 6735–6746.
25. Dessi, F., Ben-Ari, Y. & Charriaut-Marlangue, C. (1995) *Neurosci. Lett.* **201,** 53–56.
26. Sciammanna, M. A., Zinkel, J., Fabi, A. Y. & Lee, C. P. (1992) *Biochim. Biophys. Acta* **1134,** 223–232.
27. Faulk, E. A., McCully, J. D., Tsukube, T., Hadlow, N. C., Krukenkamp, I. B. & Levitsky, S. (1995) *Ann. Thorac. Surg.* **60,** 338–344.
28. Dykens, J. A. (1994) *J. Neurochem.* **63,** 584–591.
29. Reynolds, I. J. & Hastings, T. G. (1995) *J. Neurosci.* **15,** 3318–3327.
30. Dugan, L. L., Sensi, S. L., Canzoniero, L. M. T., Handran, S. D., Rothman, S. M., Lin, T.-S., Goldberg, M. P. & Choi, D. W. (1995) *J. Neurosci.* **15,** 6377–6388.
31. Newmeyer, D. D., Farschon, D. M. & Reed, J. C. (1994) *Cell* **79,** 353–364.
32. Kroemer, G., Petit, P., Zamzami, N., Vayssièrre, J.-L. & Mignotte, B. (1995) *FASEB J.* **9,** 1277–1287.
33. Mellon, P. L., Windle, J. J., Goldsmith, P. C., Padula, C. A., Roberts, J. L. & Weiner, R. I. (1990) *Neuron* **5,** 1–10.
34. Moreadith, R. W. & Fiskum, G. (1984) *Anal. Biochem.* **137,** 360–367.
35. Gochman, N. & Givelber, H. (1970) *Clin. Chem.* **16,** 229–234.
36. Skarkowska, O. & Klingenberg, M. (1963) *Biochem. Z.* **338,** 674–697.
37. Rajdev, S. & Reynolds, I. J. (1993) *Neurosci. Lett.* **162,** 149–152.
38. Smith, L. (1955) *Methods Biochem. Anal.* **2,** 427–434.
39. Ausubel, F. M., Brent, R., Kingston, R., Moore, D. D., Seidman, J. G., Smith, J. A. & Struhl, K. (1987) *Current Protocols in Molecular Biology* (Wiley, New York), pp. 2.1.1–2.2.2.
40. Cortopassi, G. A. & Arnheim, N. (1990) *Nucleic Acids Res.* **18,** 6927–6933.
41. Becker, G. L., Fiskum, G. & Lehninger, A. L. (1980) *J. Biol. Chem.* **255,** 9009–9012.
42. Fiskum, G., Craig, S. W., Decker, G. L. & Lehninger, A. L. (1980) *Proc. Natl. Acad. Sci. USA* **77,** 3430–3434.
43. Villalobo, A. & Lehninger, A. L. (1980) *J. Biol. Chem.* **260,** 7585–7590.
44. Hartley, D. M., Kurth, M. C., Bjerkness, L., Weiss, J. H. & Choi, D. W. (1993) *J. Neurosci.* **13,** 1993–2000.
45. Paraidathathu, T., de Groot, H. & Kehrer, J. P. (1992) *Free Radical Biol. Med.* **13,** 289–297.
46. Turrens, J. F., Beconi, M., Barilla, J., Chavez, U. B. & McCord, J. M. (1991) *Free Radical Res. Commun.* **12-13,** 681–689.
47. Gunasekar, P. G., Kanthasamy, A. G., Borowitz, J. L. & Isom, G. E. (1995) *J. Neurochem.* **65,** 2016–2021.
48. Boveris, A., Oschino, N. & Chance, B. (1972) *Biochem. J.* **128,** 617–630.
49. Gonzàlez-Flecha, B., Cutrin, J. C. & Boveris, A. (1993) *J. Clin. Invest.* **91,** 456–464.
50. Littauer, A. & de Groot, H. (1993) *Am. J. Physiol.* **262,** G1015–G1020.
51. Vukmanović, S. & Zamoyska, R. (1991) *Eur. J. Immunol.* **21,** 419–424.
52. Vayssière, J.-L., Petit, P. X., Risler, Y. & Mignotte, B. (1994) *Proc. Natl. Acad. Sci. USA* **91,** 11752–11756.
53. Jacobson, M. D., Burne, J. F. & Raff, M. C. (1994) *EMBO J.* **13,** 1899–1910.
54. Petit, P. X., Lecoeur, H., Zorn, E., Dauguet, C., Mignotte, B. & Gougeon, M.-L. (1995) *J. Cell Biol.* **130,** 157–167.
55. Zamzami, N., Marchetti, P., Castedo, M., Zanin, C., Vayssière, J.-L., Petit, P. X. & Kroemer, G. (1995) *J. Exp. Med.* **181,** 1661–1672.
56. Zamzami, N., Marchetti, P., Castedo, M., Decaudin, D., Macho, A., Hirsch, T., Susin, S. A., Petit, P. X., Mignotte, B. & Kroemer, G. (1995) *J. Exp. Med.* **182,** 367–377.
57. Bernardi, P., Broekemeier, K. M. & Pfeiffer, D. R. (1994) *J. Bioenerg. Biomembr.* **26,** 509–517.
58. Pastorino, J. G., Snyder, J. W., Hoek, J. B. & Farber, J. L. (1995) *Am. J. Physiol.* **268,** C676–C685.
59. Nieminen, A.-L., Saylor, A. K., Tesfai, S. A., Herman, B. & Lemasters, J. J. (1995) *Biochem. J.* **307,** 99–106.
60. Richter, C. (1993) *FEBS Lett.* **325,** 104–107.
61. Hennet, T., Bertoni, G., Richter, C. & Peterhans, E. (1993) *Cancer Res.* **53,** 1456–1460.
62. Ellerby, L. M., Ellerby, H. M., Park, S. M., Holleran, A. L., Murphy, A. N., Fiskum, G., Kane, D. J., Testa, M. P., Kayalar, C. & Bredesen, D. E. (1996) *J. Neurochem.* **67,** 1259–1267.
63. Ankarcrona, M., Dypbukt, J. M., Bonfoco, E., Zhivotovsky, B., Orrenius, S., Lipton, S. A. & Nicotera, P. (1995) *Neuron* **15,** 961–973.
64. Zamzami, N., Susin, S. A., Marchetti, P., Hirsch, T., Gómez-Monterrey, I., Castedo, M. & Kroemer, G. (1996) *J. Exp. Med.* **183,** 1533–1544.
65. Liu, X., Kim, C. N., Yang, J., Jemmerson, R. & Wang, X. (1996) *Cell* **86,** 147–157.
66. Costantini, P., Chernyak, B. V., Petronilli, V. & Bernardi, P. (1996) *J. Biol. Chem.* **271,** 6746–6751.
67. Crofts, A. R. & Chappell, J. B. (1965) *Biochem. J.* **95,** 387–392.